

D
NOSC TD 587

NOSC TD 587

Technical Document 587

OPTICAL EXTINCTION COEFFICIENTS BENEATH MARINE STRATUS CLOUDS

Comparison of coefficients calculated from
observed aerosol spectra with coefficients
specified by the Navy aerosol model

ADA132011

VR Noonkester

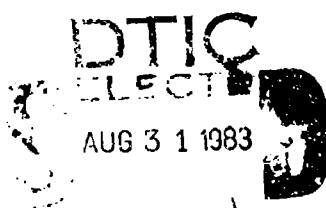
2 May 1983

Period of work: November 1982--February 1983

Prepared for
Naval Sea Systems Command
Code 62R13

Approved for public release; distribution unlimited

DTIC FILE COPY



NOSC

NAVAL OCEAN SYSTEMS CENTER
San Diego, California 92152

83 08 29 041



NAVAL OCEAN SYSTEMS CENTER, SAN DIEGO, CA 92152

A N A C T I V I T Y O F T H E N A V A L M A T E R I A L C O M M A N D

JM PATTON, CAPT, USN

Commander

HL BLOOD

Technical Director

ADMINISTRATIVE INFORMATION

Work was performed under program element 62759N, project F59551 (NOSC 532-MP33), by a member of the Tropospheric Branch (Code 5325) for Naval Sea Systems Command, Code 62R13. This document covers work from November 1982 to February 1983 and was approved for publication 2 May 1983.

Released by
JH Richter, Head
Ocean and Atmospheric
Sciences Division

Under authority of
JD Hightower, Head
Environmental Sciences
Department

CONVERSION TO SI METRIC

<u>To convert from</u>	<u>to</u>	<u>Multiply by</u>
miles (statute)	km	~ 1.61

UNCLASSIFIED

SECURITY CLASSIFICATION OF THIS PAGE (When Data Entered)

REPORT DOCUMENTATION PAGE		READ INSTRUCTIONS BEFORE COMPLETING FORM
1. REPORT NUMBER NOSC Technical Document 587 (TD 587)	2. GOVT ACCESSION NO. AD - A13201	3. RECIPIENT'S CATALOG NUMBER
4. TITLE (and Subtitle) OPTICAL EXTINCTION COEFFICIENTS BENEATH MARINE STRATUS CLOUDS Comparison of coefficients calculated from observed aerosol spectra with coefficients specified by the Navy aerosol model	5. TYPE OF REPORT & PERIOD COVERED Analysis November 1982–February 1983	
7. AUTHOR(s) VR Noonkester	6. PERFORMING ORG. REPORT NUMBER	
9. PERFORMING ORGANIZATION NAME AND ADDRESS Naval Ocean Systems Center San Diego CA 92152	8. CONTRACT OR GRANT NUMBER(s)	
11. CONTROLLING OFFICE NAME AND ADDRESS Naval Sea Systems Command, Code 62R13 Washington DC 20362	10. PROGRAM ELEMENT, PROJECT, TASK AREA & WORK UNIT NUMBERS PE 62759N Proj FS9551 (NOSC 532-MP33)	
14. MONITORING AGENCY NAME & ADDRESS (if different from Controlling Office)	12. REPORT DATE 2 May 1983	
	13. NUMBER OF PAGES 30	
16. DISTRIBUTION STATEMENT (of this Report)	15. SECURITY CLASS. (of this report) Unclassified	
	15a. DECLASSIFICATION/DOWNGRADING SCHEDULE	
17. DISTRIBUTION STATEMENT (of the abstract entered in Block 20, if different from Report)		
18. SUPPLEMENTARY NOTES		
19. KEY WORDS (Continue on reverse side if necessary and identify by block number) Optical extinction coefficients Marine aerosol spectra Maritime stratus cloud layers Electro-optical path characteristics Meteorological models		
20. ABSTRACT (Continue on reverse side if necessary and identify by block number) Vertical profiles of extinction coefficients for wavelengths of 0.53, 3.75, and 10.59 μm were calculated from observed profiles of the liquid water aerosol spectra in marine stratus layers. These profiles were obtained for air masses characterizing marine and continental air masses. A recently developed Navy aerosol model specifies optical extinction by aerosols at the surface as a function of wind speed, relative humidity (less than saturated), and air mass type. The capability of the model to duplicate the observed profiles below cloud base was determined. The surface model was applied to the above-surface conditions by assuming various vertical profiles of relative	(Continued on reverse side)	

UNCLASSIFIED

SECURITY CLASSIFICATION OF THIS PAGE (When Data Entered)

20. Continued

humidity below cloud base. Comparison of the observed and model profiles were made for various combinations of surface wind speed, humidity profiles, and air mass type. These comparisons indicated that the model could not reproduce the observed profiles of optical extinction by aerosols below marine stratus clouds.

Accession For	
NAME	Crew
DATE	10/10/01
UNCLASSIFIED	<input type="checkbox"/>
Justification	
PV	
Distribution	
Availability Codes	
Avail and/or	
DIST	Special
A	



S-N 0102-LF-014-6601

UNCLASSIFIED

SECURITY CLASSIFICATION OF THIS PAGE (When Data Entered)

CONTENTS

1. INTRODUCTION . . . page 2
 2. NAVY AEROSOL MODEL . . . 3
 3. STRATUS LAYER DATA . . . 4
 - a. Sensors . . . 4
 - b. Data acquisition . . . 5
 - c. Spectral data. . . 6
 4. AIR MASS FOR STRATUS DATA . . . 6
 - a. N and \bar{r} . . . 6
 - b. Mode in $n(r)$. . . 8
 - c. Air mass source . . . 9
 5. PROFILE OF $k(\lambda)$ BENEATH STRATUS . . . 11
 - a. Relation between $k(\lambda)$ and w^* . . . 11
 - b. Average profile of w^* and $k(\lambda)$ beneath stratus base . . . 12
 6. PROFILE OF RELATIVE HUMIDITY . . . 13
 7. SURFACE WIND SPEED . . . 15
 8. PROFILES OF MODEL $k(\lambda)$ s . . . 15
 - a. Graphical presentation . . . 15
 - b. Variation of $k(\lambda)$ with air mass . . . 16
 - c. Vertical gradient of modeled $k(\lambda)$. . . 16
 - d. Relative contribution of each mode to $k(\lambda)$. . . 16
 9. CRITERIA FOR ACCEPTANCE OF MODEL . . . 18
 - a. "Acceptable" test . . . 18
 - b. Likely error in observed $k(\lambda)$ s . . . 18
 - c. Vertical profiles of observed $k(\lambda)$ s . . . 19
 - d. Model acceptance test using profiles of $k(\lambda)$ s . . . 19
 10. COMPARISON OF MODELED AND OBSERVED $k(\lambda)$ PROFILES . . . 19
 11. COMPARISON OF MODELED AND OBSERVED $n(r)$. . . 20
 12. SUMMARY AND CONCLUSIONS . . . 23
 - REFERENCES . . . 25
- APPENDIX A: COMPARISON OF MODELED AND OBSERVED $k(\lambda)$ PROFILES . . . 27

1. INTRODUCTION

Methods of specifying optical extinction coefficients, k , (visible through infrared) in the marine boundary layer through the use of meteorological observables are needed to support naval electro-optical systems. The k -coefficient is a function of wavelength, λ , and atmospheric water content in both condensed form and vapor. The concentration of condensation in the form of aerosols is usually quantitatively depicted by a spectrum, $n(r)$, where r is aerosol radius. Coefficient $k(\lambda)$ is critically dependent on the distribution of the total particle number, N , within $n(r)$.

Most data on $n(r)$ in the marine boundary layer have been obtained near the surface. Published, readily usable models specifying $n(r)$ (eg, Wells et al, 1977, and a Navy model described by Noonkester, 1980) have been developed primarily from the surface data. A recently developed model specifying $n(r)$ and $k(\lambda)$ (Gathman, 1983) has been accepted as a replacement of an earlier Navy model (described by Noonkester, 1980) for naval EO applications. This Navy aerosol model, hereafter called "Navy model" or "model," was based primarily on near-surface data, is readily usable, and is being tested for various meteorological conditions.

Some Navy aerosol systems will depend on optical paths that have an appreciable portion above the surface; and to be acceptable, a model must be successful for the above-surface needs. Recent acquisition of data by NOSC (Noonkester, 1982a, 1982b) provides an opportunity to test the model for above-surface optical paths. These data are detailed observations of $n(r)$ at many levels in maritime stratus cloud layers. Because stratus clouds are common over large regions of the ocean, capping layers containing numerous aerosols, they pose a likely limiting environment for systems. The purpose of this document is to compare $k(\lambda)$'s specified by the model with $k(\lambda)$'s calculated from the observed $n(r)$'s beneath stratus clouds. A comparison of $n(r)$'s specified by the model with observed $n(r)$'s is made to isolate reasons for differences between the modeled and observed $k(\lambda)$'s. These comparisons indicate that the model cannot specify $n(r)$ and $k(\lambda)$ beneath stratus clouds. Apparently the model must be modified appreciably before it can be applied to conditions beneath stratus clouds.

2. NAVY AEROSOL MODEL

The Navy model (Gathman, 1983) consists of a three-mode, log-normal distribution of $n(r)$ used in conjunction with Mie-theory calculations to specify $k(\lambda)$ for 40 λ s in the range $0.20 \mu\text{m} \leq \lambda \leq 40.0 \mu\text{m}$. The real and imaginary parts of the refractive index are specified. The model also specifies the water vapor absorption for the 40 λ s, although that characteristic is not used here.

The basic contents of the model for the condensed portion of the atmospheric water content are as follows:

$$k(\lambda) = 10^{-3} \pi \int Q(\lambda, m) n(r) r^2 dr \quad (1)$$

$$n(r) = \sum_{i=1}^3 A_i e^{-\ln^2 \left(\frac{r}{r_i} \right)}, \quad (2)$$

where $n(r)$ is in $\text{cm}^{-3} \mu\text{m}^{-1}$ and $k(\lambda)$ is in km^{-1} . Also

Q = nondimensional extinction cross section for spherical particles

m = refractive index, both real and imaginary parts

$A_1 = 2000(\text{AM})^2$ [AM = air mass parameter, in values of 1-10. AM = 1 for open ocean; AM = 10 for coastal region.]

A_2 = the maximum of 0.5 or $5.866(w - 2.2)$

$A_3 = \text{the maximum of } 1.4 \times 10^{-5} \text{ or } 0.01527(w' - 2.2)$

w = 24-hour average surface wind speed, in m/s

w' = current surface wind speed, in m/s

$F = \frac{2 - f}{6(1 - f)}^{1/3}$ (growth factor)

r_i = dry particle size for mode i

$r_1 = 3.0 \times 10^{-2} \mu\text{m}$

$r_2 = 2.4 \times 10^{-1} \mu\text{m}$

$r_3 = 2.0 \mu\text{m}$

f = fractional relative humidity

A_1 , A_2 , and A_3 correspond respectively to modes 1, 2, and 3.

One convenient form of $k(\lambda, t)$ is as follows:

$$k(\lambda, f) = \frac{10^{-3} \pi}{F(f)} \sum_{i=1}^3 A_i 10^{C_i(\lambda, f)} . \quad (3)$$

Tabulations of C_i are available for the 40 λ s at f_s of 0.50, 0.85, 0.95, and 0.99. Absorption by water vapor was not considered here.

When w and w' are not known, the model provides "default" values as follows:

Tropical	$w = w' = 4.1 \text{ m/s}$
Mid-latitude summer	$w = w' = 4.1 \text{ m/s}$
Mid-latitude winter	$w = w' = 10.3 \text{ m/s}$
Subarctic summer	$w = w' = 6.7 \text{ m/s}$
Subarctic winter	$w = w' = 12.4 \text{ m/s}$

Although the Navy model was designed for near-surface conditions, the model was applied to above-surface stratus layer conditions by using f as an independent variable. Because f errors were unknown during the stratus measurements, the f measurements were not used to establish elevations for comparison. Although an adiabatic vertical profile of f was used to provide the elevation dependence for the model, this assumption is not critical for these comparisons.

C. STRATUS LAYER DATA

a. SENSORS

Measurements made aboard a twin-engine Piper Navajo flying at 54 m/s included elevation, z , temperature, T , dew point, T_d , and $n(r)$. The combined use of radar and pressure altimeters reduced measurement errors in z to less than $\pm 3 \text{ m}$ up to 700 m. The total system accuracy of the T and T_d measurements has not been finalized. A PMS ASSP-100 spectrometer provided $n(r)$ over the

range $0.23 \mu\text{m} \leq r \leq 14.7 \mu\text{m}$, and a PMS OAP-200 spectrometer provided $n(r)$ over the range $14.2 \mu\text{m} \leq r \leq 150 \mu\text{m}$. T and z were sampled every 5 s and a complete $n(r)$ was obtained every 8 s.

b. DATA ACQUISITION

Slow descents were made through extensive stratus cloud decks, to estimate the elevations of the cloud tops, z_t , and cloud bases, z_c . Horizontal runs of 2 minutes (6.44 km) were then made at about the following elevations:

z_0 (near surface)
 $0.2z_c$
 $z_c/2$
 $z_c - 80 \text{ m}$
 $z_c - 60 \text{ m}$
 $z_c - 40 \text{ m}$
 $z_c - 20 \text{ m}$
 z_c
 $z_c + 20 \text{ m}$
 $z_c + 40 \text{ m}$
 $(z_c + z_t)/2$ [midcloud]
 $z_t - 40 \text{ m}$
 z_t
 $z_t + 40 \text{ m}$

All runs were made both into and with the estimated surface wind.

The maximum and minimum standard deviations of z were respectively 9.3 and 1.6 m, and the average standard deviation was 4.7 m. All data along a horizontal run were accepted if they were acquired at an elevation within $\pm 7 \text{ m}$ of the average.

c. SPECTRAL DATA

Measurements of the number, n , of aerosols in a volume of 1 cm^3 for a bandwidth of $1 \mu\text{m}$ centered at a radius r_i were made every 8 s during each 2-min horizontal run. A complete spectrum, $n(r)$, consisted of 47 $n(r_i)$ s. An average $n(r_i)$ in each radius band was obtained by averaging all $n(r_i)$ s observed during each 2-min run. Each 8-s spectrum represented 429 m, and the 2-min average $n(r)$ represented 6.44 km, or fifteen 8-s spectra.

Parameters calculated from the average $n(r)$ include (1) the total number of particles, N , (2) the mean radius, \bar{r} , (3) the liquid water content, w^* , and (4) $k(\lambda)$ for λ s of 0.53, 3.75, and $10.59 \mu\text{m}$. The following equation was used to calculate w^* :

$$w^* = \frac{4}{3} \pi D \int r^3 n(r) dr , \quad (4)$$

where D is the density of pure water, in g/cm^3 . $k(\lambda)$ was calculated from equation (1). The aerosols were assumed to be spherical, and the integration was extended over the range $0.23 \mu\text{m} \leq r \leq 150 \mu\text{m}$. The refractive indices used are those given by Selby et al (1976). The model used another set of refractive indices. The $k(\lambda)$ s calculated from the observed $n(r)$ s will be called observed $k(\lambda)$ s, although optical extinctions were not observed.

Stratus layer aerosol data were obtained over the ocean about 80 miles southwest of San Diego on 14, 28, and 29 May and 11, 13, 14, 17, and 18 August 1981. Figure 1 gives the measurement levels and the cloud-top and cloud-base elevations on each day of the measurements. The cloud base was defined to be at the level where $w^* = 0.02 \text{ g/m}^3$, as discussed in section 5b.

4. AIR MASS FOR STRATUS DATA

a. N AND \bar{r}

Table 1 gives N and \bar{r} at the surface and at 100 m above the cloud bases for the May and August data. N was greater during August at all levels. N

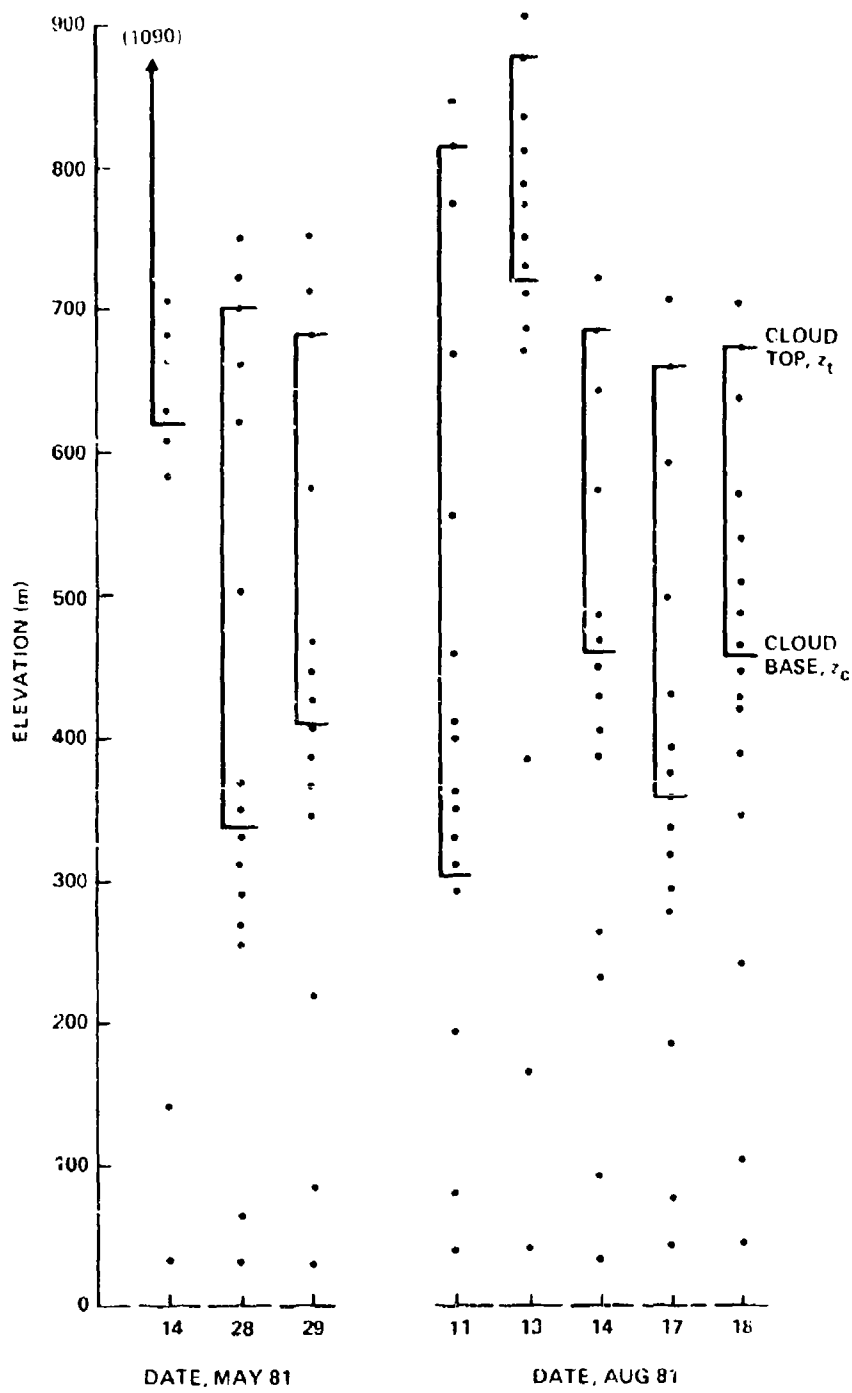


Figure 1. Elevation of horizontal runs by NOSC airborne sensor system. Region of cloud deck is shown for each day of measurement.

was about 2.5 times greater during August at 100 m above cloud base. The mean radius, \bar{r} , was larger at all elevations during May. Pruppacher and Klett (1978) give N values about four times greater in continental clouds than in marine clouds at $r > 3 \mu\text{m}$ and give examples showing that $n(r)$'s are characterized by large \bar{r} 's in marine air masses. Accordingly, the May and August data could be considered to represent marine and continental air masses, respectively.

Data Period	Near Surface			100 m above Cloud Base		
	N (cm ⁻³)	\bar{r} (cm)	w* (g/m ³)	N (cm ⁻³)	\bar{r} (cm)	w* (g/m ³)
1981						
May: 3 days	62	0.67	3.6×10^{-4}	269	4.0	0.15
August: 5 days	84	0.39	9.4×10^{-5}	665	3.1	0.21

Table 1. Average aerosol spectrum parameters representing a horizontal distance of 6.44 km.

b. MODE IN $n(r)$

In the May data, distinct modes formed in $n(r)$ above the cloud base. The aerosol radius at the peak of the mode increased linearly with elevation from 3 μm near cloud base to a maximum just below cloud top. Modes did not form in the clouds during August, apparently because a much greater number of cloud condensation nuclei were present that were capable of competing for the available moisture. Nieburger and Chien (1960), Fitzgerald (1974), and Lee et al (1980) presented cloud models that produced modes in $n(r)$ for marine air masses.

c. AIR MASS SOURCE

The measurement region was near 118°W longitude and 32°N latitude, as shown in figure 2. An average surface pressure map was constructed for the region bounded by longitudes from 110° to 140° west and latitudes from 30° to 55° north. Pressures were taken from the 0400 PST synoptic maps at intersections of 5° longitude and latitude increments within this region for the days 13, 14, 27, 28, and 29 May, to represent the May data, and 10, 11, 12, 13, 14, 16, 17, and 18 August, to represent the August data. After average pressures were computed for each intersection, maps of the average pressures were constructed for the May and August days, and these are presented in figure 2. The average pressure map for May shows an offshore subtropical high in a southerly position and a low adjacent to the northwest part of the region. During August the average pressure map shows a subtropical high elongated north to south in the western portion of the region, producing a northerly flow west of 120° longitude at all latitudes.

The northerly flow at all latitudes in figure 2 for the August days provides strong evidence that a continental air mass would be present during the August measurement days. Because the pressure patterns are highly similar for the May and August days along the coast of California, a continental air mass might be expected at the measurement site during May. However, the west-east pressure gradient is greater during May west of San Diego. A stronger cross-isobaric flow (more westerly wind) is expected in the San Diego region when the west-east pressure gradient increases. The stronger west-east pressure gradient for the May days might have been sufficient to maintain a marine air mass in the measurement region during May.

Taken collectively, the above data give strong evidence toward the conclusion that the aerosols had a continental source during the August days and give appreciable evidence toward the conclusion that the aerosols had a marine source during the May days. Accordingly, air mass parameters (AM) of 1 and 10 will be assigned to the May and August days, respectively. Subsequent discussions will show that the AM value assignments were not critical in the comparisons.

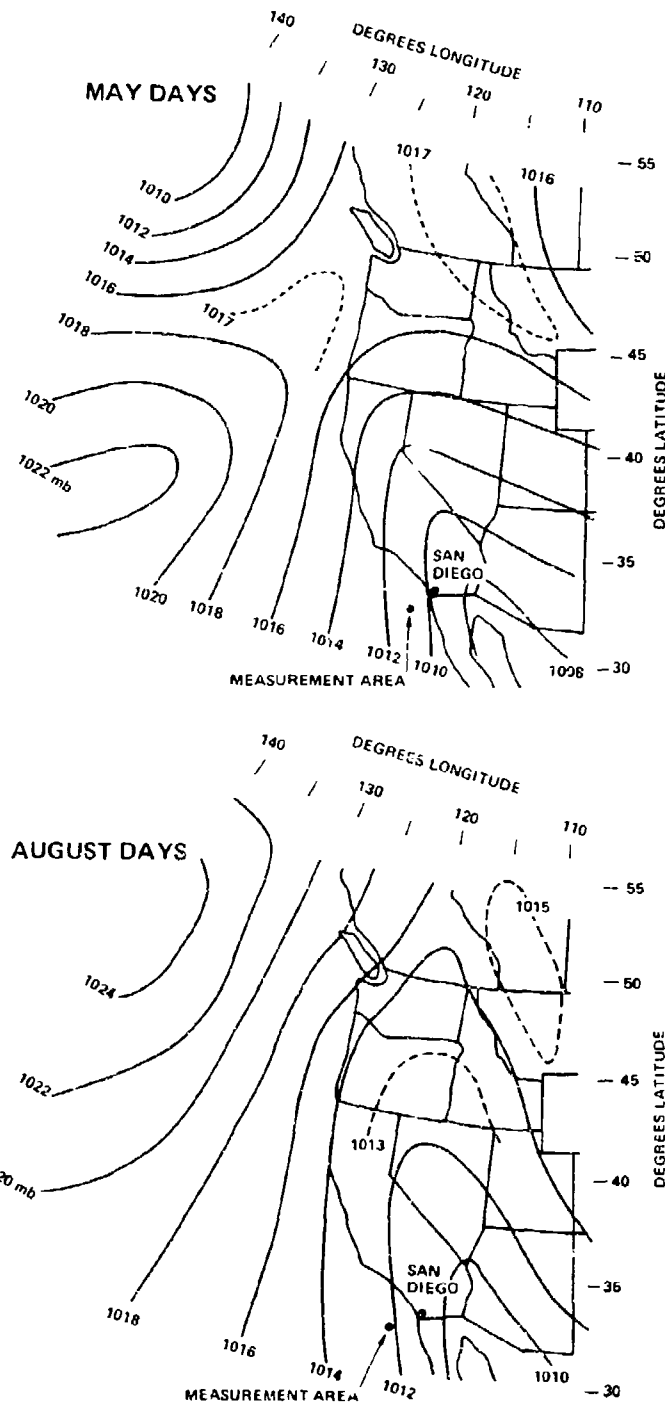


Figure 2. Representative surface pressure patterns for measurement days in May and August 1981. The measurement area location, near San Diego, is shown. The pressure patterns indicate a probable continental air mass present in the measurement area in August, a probable marine air mass in May.

5. PROFILE OF $k(\lambda)$ BENEATH STRATUS

a. RELATION BETWEEN $k(\lambda)$ AND w^*

When $k(\lambda)$ and w^* are determined from $n(r)$ by means of equations (1) and (4) respectively and the coefficients a and b in the expression

$$k(\lambda) = a(w^*)^b \quad (5)$$

are determined by statistical regression analysis, the coefficient of correlation, ρ , between $k(\lambda)$ and $a(w^*)^b$ is found to be greater than 0.95 for a great variety of spectral shapes. The coefficients a and b vary with λ and appear to vary with air mass (eg, Pinnick et al, 1979; Hughes and Jensen, 1978; Neonkester, 1980).

Comparisons of the modeled and observed $k(\lambda)$'s were made for λ s of 0.53, 3.75, and 10.59 μm . Table 2 gives a , b , and ρ for these λ s determined from $n(r)$ stratus data except $n(r)$ where N was less than $10/\text{cm}^3$, with the May and August days considered separately. The large ρ s indicate that w^* can almost exactly specify $k(\lambda)$ in equation (5).

Data Period	λ (μm)	a	b	Correlation Coefficient, ρ
May: 3 days	0.53	194	0.834	0.99
	3.75	308	0.950	0.99
	10.59	308	1.16	1.00
August: 5 days	0.53	231	0.796	0.99
	3.75	351	0.949	0.98
	10.59	282	1.13	1.00

Table 2. Values of a and b in equation (5) determined by regression analysis. $k(\lambda)$ has units km^{-1} for these constants.

b. AVERAGE PROFILE OF w^* AND $k(\lambda)$ BENEATH STRATUS BASE

If the average vertical profile of w^* below cloud base is known for the May and August data, then the average vertical profile of $k(\lambda)$ below cloud base can be obtained from equation (5) by using values of a and b in table 2.

The bases of the stratus clouds could not be uniquely determined visually because the decrease in horizontal visibility from "good" to "poor" was gradual and extended over depths ranging from 40 to 100 m during ascent into the clouds. The bases of the stratus clouds were assumed to be at the level where $w^* = 0.02 \text{ g/m}^3$. When the average cross-sectional aerosol area at this level and Koschmieder's equation are used, the level chosen for cloud base has a visibility of 435 m. According to the international visibility code, this visibility corresponds to a moderate fog.

Figure 3 presents the average w^* below the cloud base ($w^* = 0.02 \text{ g/m}^3$) for the May and August days. Distances relative to this defined cloud base will be identified by z^* .

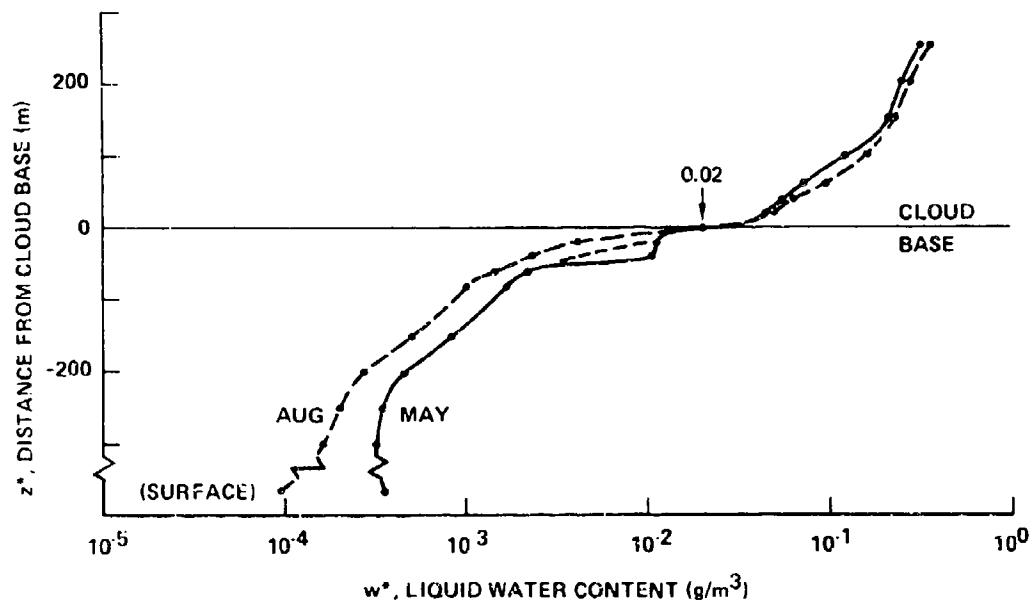


Figure 3. Profile of the average liquid water content for 3 stratus days in May 1981 (marine air mass) and for 5 stratus days in August 1981 (continental air mass).

The minimum w^* has been reported to range from 0.01 to 0.05 g/m³ near the base of stratiform clouds (Houghton, 1951) and in fogs (McCartney, 1976; Heaps, 1982). Using this range of w^* 's, the cloud-base heights would be in the range -10 m < z^* < 20 m in figure 3. The increase in w^* above $z^* = 20$ m is linear, commensurate with moist adiabatic cooling and cloud-top entrainment. Apparently, the level at which $w^* = 0.02$ g/m³ is near the saturation level ($f = 1.0$). The level where $w^* = 0.02$ g/m³ is considered to be within ± 15 m of the true saturation level.

In figure 3, the larger values of w^* below cloud base for May would be expected because r is greater at all levels. The near-constant value of w^* between $z^* = -20$ m and $z^* = -40$ m for May was caused by a perturbation in the data at one level on 29 May and is not considered to be representative; the dashed portion is a more likely w^* profile during May in this region. The more rapid increase of w^* in the region -40 m < $z^* < 0$ during August is considered to be caused by the large uptake of water vapor by a greater number of small aerosols as saturation is approached.

In equation (5), $k(\lambda, z^*)$ can be determined by using $w^*(z^*)$'s from figure 3. Figure 4 gives the observed $k(z^*)$'s for λ 's of 0.53, 3.75, and 10.59 μm separately for the May and August days.

6. PROFILE OF RELATIVE HUMIDITY

The model is effective in providing $k(\lambda)$ as a function of elevation, z , if the fractional relative humidity, f , can be specified as a function of elevation. Thus, if f can be specified as a function of distance below z^* , the $k(\lambda)$'s given by the model can be compared with the $k(\lambda, z^*)$'s given in figure 4.

Observations and theory show that the region below the cloud base approximates a well-mixed adiabatic layer. Because errors in the f 's measured below the stratus clouds along the runs are unknown and may be large at $f > 0.9$, the deviations of the actual $f(z^*)$'s from those in an adiabatic layer cannot be determined. An adiabatic lapse rate for f will be assumed to be present below

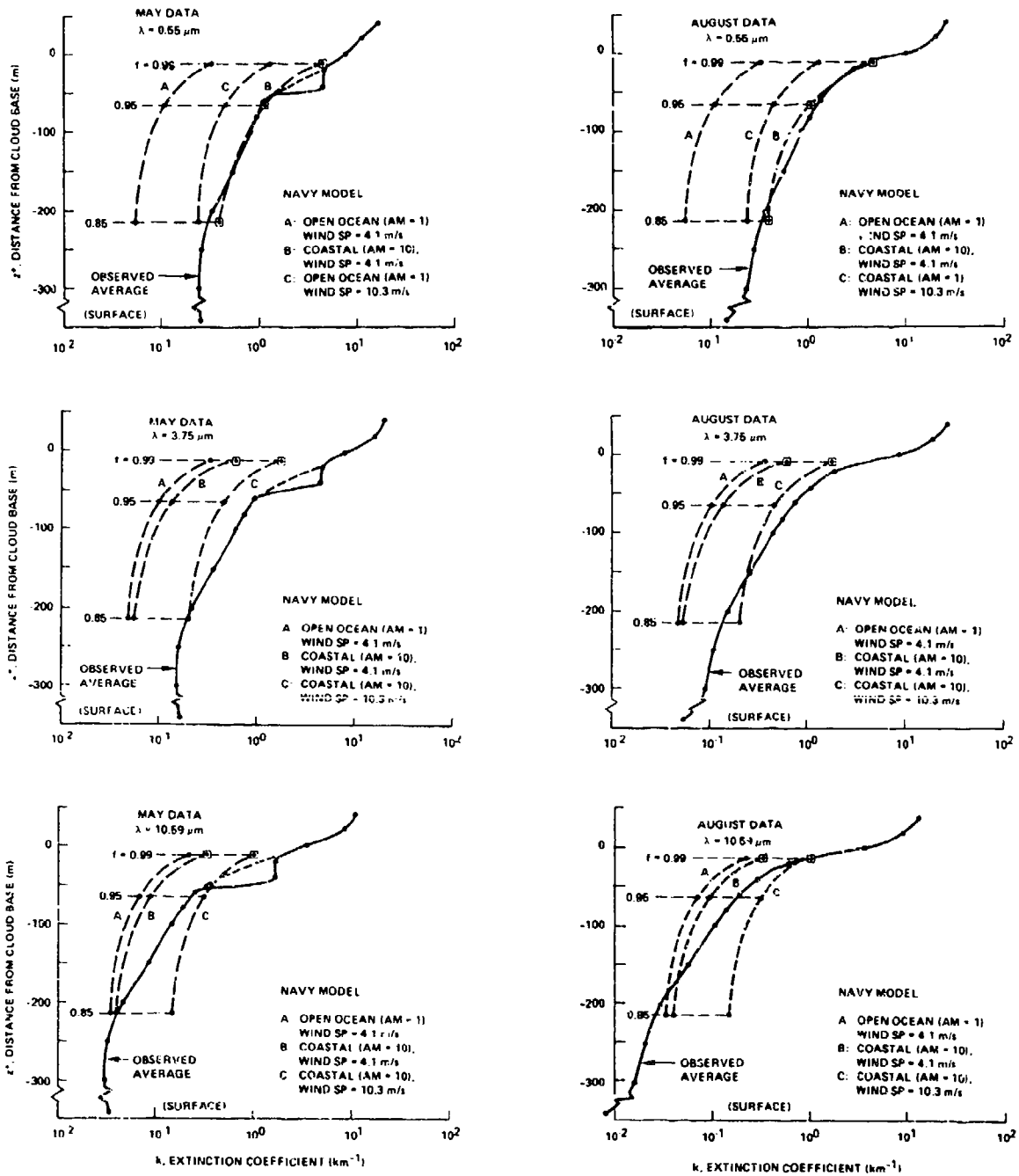


Figure 4. Profiles of optical extinction coefficients by aerosols for observations (solid) and for the Navy model (dashed). In the Navy model, profile A represents open ocean ($AM = 1$) with 4.1 m/s wind speed, profile B represents coastal ($AM = 10$) with 4.1 m/s wind speed, and profile C represents either open ocean ($AM = 1$) or coastal ($AM = 10$) with 10.3 m/s wind speed.

cloud base, and f will be assumed to be 1.0 at the cloud base. The z^* 's for f_s of 0.99, 0.95, and 0.85 in an adiabatic layer, corresponding to f_s for the tabulated C_i 's in equation (3), are respectively -12, -65, and -215m. Data shown in a later section will demonstrate that large changes in the profile of f would not permit the model to approximate the observed $k(\lambda)$'s; thus an assumption of an adiabatic lapse rate for f is reasonable.

7. SURFACE WIND SPEED

The 24-hour average surface wind speed, w , and the current surface wind speed, w' , are the two remaining parameters unspecified in the model. Observations by the author during the low-level horizontal runs indicated that w' ranged from about 5 to 12 knots (2.5 to 6 m/s) on all 8 days. The synoptic patterns near the observation days indicated that the local wind speed should be representative of a large region; thus the current and 24-hour average wind speed can be assumed to be the same. Acceptance of the default wind speeds w and w' of 4.1 m/s for a midlatitude summer appears reasonable.

8. PROFILES OF MODEL $k(\lambda)$ 'S

a. GRAPHICAL PRESENTATION

Figure 4 presents model-provided $k(\lambda, z^*)$'s appropriate for an adiabatic lapse rate for f below the stratus cloud base. The model $k(\lambda, z^*)$ profiles are presented separately for λ 's of 0.55, 3.75, and 10.59 μm and for the May and August data. For comparison, model $k(\lambda, z^*)$'s are given for AMs of 1 and 10 on all figures (although AMs of 1 and 10 are considered to be appropriate for May and August, respectively). The k_s calculated from the stratus data for $\lambda = 0.53 \mu\text{m}$ should be comparable to k_s tabulated for the model at $\lambda = 0.55 \mu\text{m}$. Hereinafter, the observed k for $\lambda = 0.53 \mu\text{m}$ will be considered applicable to $\lambda = 0.55 \mu\text{m}$.

b. VARIATION OF $k(\lambda)$ WITH AIR MASS

The difference between the model k_s for AMs of 1 and 10 increases with an increase of f_s and with a decrease in λ . The differences are appreciable for $\lambda = 0.55 \mu\text{m}$. The differences at λ_s of 3.75 and 10.59 μm may be insignificant for many purposes.

c. VERTICAL GRADIENT OF MODELED $k(\lambda)$

The vertical gradients ($\Delta k / \Delta z^*$) for the model were calculated for the change in k between f_s of 0.99 and 0.95 and between f_s of 0.95 and 0.85. The vertical gradients were greater for the larger f_s and for the AM of 10. For either AM, the gradients decreased in the following order of λ_s : 3.75, 0.55, 10.59 μm . The variation with λ for an AM of 1 was minor. The greatest increase in the vertical gradient of k for any λ was 16; it occurred for a λ of 0.55 μm when AM changed from 1 to 10 at the large f_s .

d. RELATIVE CONTRIBUTION OF EACH MODE TO $k(\lambda)$

Comparison of the relative contribution of each mode of the aerosol model to the extinction coefficient $k(\lambda)$ permits evaluation of the significance of the air mass factor through the use of A_1 , the average 24-hour wind speed through the use of A_2 , and the current wind speed through the use of A_3 . Table 3 gives the percent contribution of each mode to $k(\lambda)$ for λ_s of 0.55, 3.75, and 10.59 at f_s of 0.99, 0.95, 0.85, and 0.50 in an open ocean (AM = 1) and a coastal environment (AM = 10) when the surface wind speed (current and 24-hour average) is 4.1 m/s.

Data in table 3 indicate the following:

- (1) For AM = 1, mode 3 is most important and mode 1 may be ignored. For AM = 10, mode 1 controls $k(\lambda)$ for $\lambda = 0.55 \mu\text{m}$ and all three modes must be used for λ_s of 3.75 and 10.59 μm .

λ (μm)	f	Open Ocean (AM = 1)			Coastal (AM = 10)		
		Contribution (%)			Contribution (%)*		
		Mode 1	Mode 2	Mode 3	Mode 1	Mode 2	Mode 3
0.55	0.99	13	36	51	(94)	(3)	(4)
	0.95	9	39	52	(91)	(4)	(5)
	0.85	6	41	53	(86)	(6)	(8)
	0.50	4	43	53	(81)	(9)	(10)
3.75	0.99	1	43	56	(47)	(23)	(30)
	0.95	0	35	65	21	28	51
	0.85	0	27	73	11	24	65
	0.50	0	20	80	6	19	75
10.59	0.99	0	17	83	(31)	(11)	(58)
	0.95	0	10	90	21	8	71
	0.85	0	8	92	16	6	78
	0.50	0	5	95	9	5	86

*Parentheses are used to indicate where mode 1 contributes more than 25% to total k .

Table 3. Percent contribution of each mode to $k(\lambda)$ for the Navy aerosol model in open-ocean and coastal environments for a wind speed of 4.1 m/s (aerosols only).

- (2) The change in the contribution of the modes as AM, f, and λ change is less distinct for mode 2. For either AM, mode 2 increases in importance as f decreases at $\lambda = 0.55 \mu\text{m}$ and decreases in importance as f decreases for $\lambda_s = 3.75$ and $10.59 \mu\text{m}$. Mode 2 contributes about the same for any AM when $\lambda = 10.59 \mu\text{m}$.
- (3) For either AM, mode 3 increases in importance as f decreases and as λ increases. Mode 3 is more important than mode 2 for any f.

In general, these features indicate that the importance of the smallest aerosols (mode 1) increases as f increases and as λ decreases, and that the importance of large aerosols (mode 3) increases as f decreases and as λ increases. These general relations are expected. The relative intermediate importance of mode 2 for an AM of 10 may not have been expected.

Because mode 1 includes many aerosols in the radius region below the minimum observed radius ($r = 0.23 \mu\text{m}$), comparison of the observed and modeled $k(\lambda)$ is not appropriate when the relative contribution of mode 1 to $k(\lambda)$ is appreciable. An appreciable contribution for mode 1 is arbitrarily considered to occur when the relative contribution of mode 1 to k is 25 percent or more of the total k . All affected modes in this category are enclosed by parentheses in table 3. All f_s and λ_s in table 3 are acceptable for comparison for an open-ocean environment. In a coastal environment, only λ_s of 3.75 and $10.59 \mu\text{m}$ at f_s of 0.95, 0.85, and 0.50 are acceptable for comparison. In figure 4, the data points of the modeled $k(\lambda)$'s in which mode 1 contributes 25 percent or more to the total value are enclosed by squares and will not be considered in the comparisons.

9. CRITERIA FOR ACCEPTANCE OF MODEL

a. "ACCEPTABLE" TEST

A rigid test of the model would require accurate observations of $n(r)$ along with accurate measurements of f , w , and w' and an appropriate method of obtaining AM. Reliable differences between the observed and the modeled $n(r)$'s or $k(\lambda)$'s could then be determined. The significance of the difference between the modeled and observed $k(\lambda)$'s could be estimated relative to an optical system application if criteria for successful performance of the system are quantified. Application of this procedure is unlikely since accuracies of the observed $n(r)$'s are generally unknown, a method of obtaining AM is not defined, and system performance limitations by errors in $k(\lambda)$ are not usually available.

b. LIKELY ERROR IN OBSERVED $k(\lambda)$ 'S

Simultaneous measurements by colocated PMS aerosol measuring devices at the NW tip of San Nicolas Island during a 9-day period in May 1979 when atmospheric conditions varied considerably showed that the $k(\lambda)$'s calculated from the observed $n(r)$'s differed by a factor of 2 to 3. $k(\lambda)$'s determined by a nearby nephelometer were within a factor of 2 to 3 of the $k(\lambda)$'s calculated

from the observed $n(r)$ s (Jensen, 1980). Thus the $k(\lambda)$ s in figure 4, obtained from the average w_s , should be within a factor of 2 to 3 of values expected from measurements by similar devices and could be within a factor of 2 to 3 of the real values in a representative stratus-cloud layer. Accordingly, the modeled and observed $k(\lambda)$ s can be considered to have appreciable differences when they differ by a factor of more than 3.

c. VERTICAL PROFILES OF OBSERVED $k(\lambda)$ s

No evidence has been found to indicate that any systematic errors in the measurements of $n(r)$ by the same PMS spectrometer vary within a period of several weeks. Changes in the observed $n(r)$ from the data period in May to August can be considered real. The vertical profiles of the observed $k(\lambda)$ s in figure 4 are considered to approximate the true profile closely, although the magnitude of the $k(\lambda)$ s may be systematically too large or too small by a factor of 2 to 3.

d. MODEL ACCEPTANCE TEST USING PROFILES OF $k(\lambda)$ s

The true profile of f may not approximate an adiabatic layer (for which $f = 1$ at the level where $w^* = 0.02 \text{ g/m}^3$), as assumed in the construction of the profile of the modeled $k(\lambda)$ s in figure 4. The modeled $k(\lambda)$ profiles would be acceptable if reasonable changes in the assumed vertical profile of f would cause the modeled $k(\lambda)$ s to be within a factor of 3 of the observed $k(\lambda)$ profiles at all levels and λ s and for reasonable values of w , w' , and AM . A vertical gradient of f greater than adiabatic would not be reasonable, whereas a profile of f less than adiabatic might be acceptable when $f = 1$ is within $\pm 15 \text{ m}$ of $z^* = 0$. The vertical adiabatic gradient of f is about $+1.4\% / 20 \text{ m}$ for the temperatures on the days of measurement.

10. COMPARISON OF MODELED AND OBSERVED $k(\lambda)$ PROFILES

Appendix A is a detailed comparison stating that the model $k(\lambda)$ s cannot simultaneously approximate (within a factor of 3) the observed $k(\lambda)$ s for all λ s, both months, and all elevations - even with unreasonable changes in the

profile of relative humidity and surface wind speeds (w and w'). This conclusion applies as well to the surface, where the model would be expected to be reliable.

11. COMPARISON OF MODELED AND OBSERVED $n(r)$

Comparison of the modeled and observed $n(r)$ for selected values of AM and f should reveal some reasons for the large differences in the modeled and observed $k(\lambda)$ s. The default wind speed of 4.1 m/s given by the model for a midlatitude summer appears reasonable for the synoptic patterns prevalent during May and August 1981. Reasons given in section 4 support selection of the model "open ocean" (AM = 1) to represent the May data and "coastal" (AM = 10) to represent the August data.

Figures 5 and 6 present the modeled and observed $n(r)$ for f_s of 0.99, 0.95, and 0.85. Figure 5 is for the May data and figure 6 is for the August data. The left part of figures 5 and 6 provides the contribution of each mode of the model to $n(r)$ at an f of 0.99 for the May and August data, respectively.

Compared to the observed $n(r)$, the modeled $n(r)$ provides considerably fewer (as few as 1/10 the total) aerosols roughly in the region $0.4 \mu\text{m} < r < 10 \mu\text{m}$ for May and fewer aerosols (as few as 1/5 the total) roughly in the region $1 \mu\text{m} < r < 10 \mu\text{m}$ for August. The model overestimates $n(r)$ for $r > 20 \mu\text{m}$ at $f = 0.99$ for both months. The large positive departure of the observed $n(r)$ above the model for May at $f = 0.85$ (surface) in the region $r > 40 \mu\text{m}$ is appreciable.

The most significant and consistent differences between the modeled and the observed $n(r)$ are roughly in the radius region centered between 1 and 3 μm for May and between 2 and 4 μm for August. The observed $n(r)$ s are similar for May and August when $f = 0.95$ in the region $r > 3 \mu\text{m}$. $n(r)$ is about $40 \text{ cm}^{-3} \mu\text{m}^{-1}$ at $r \approx 3 \mu\text{m}$ for both months. Given $AM = 10$, $w = 10.3 \text{ m/s}$ (20 knots), $w' = 15.5 \text{ m/s}$ (30 knots), and $f = 0.99$, the model yields $n(r)$ (for $r = 3 \mu\text{m}$) = $4.4 \text{ cm}^{-3} \mu\text{m}^{-1}$. Thus, the model appears incapable of producing the observed $n(r)$ in

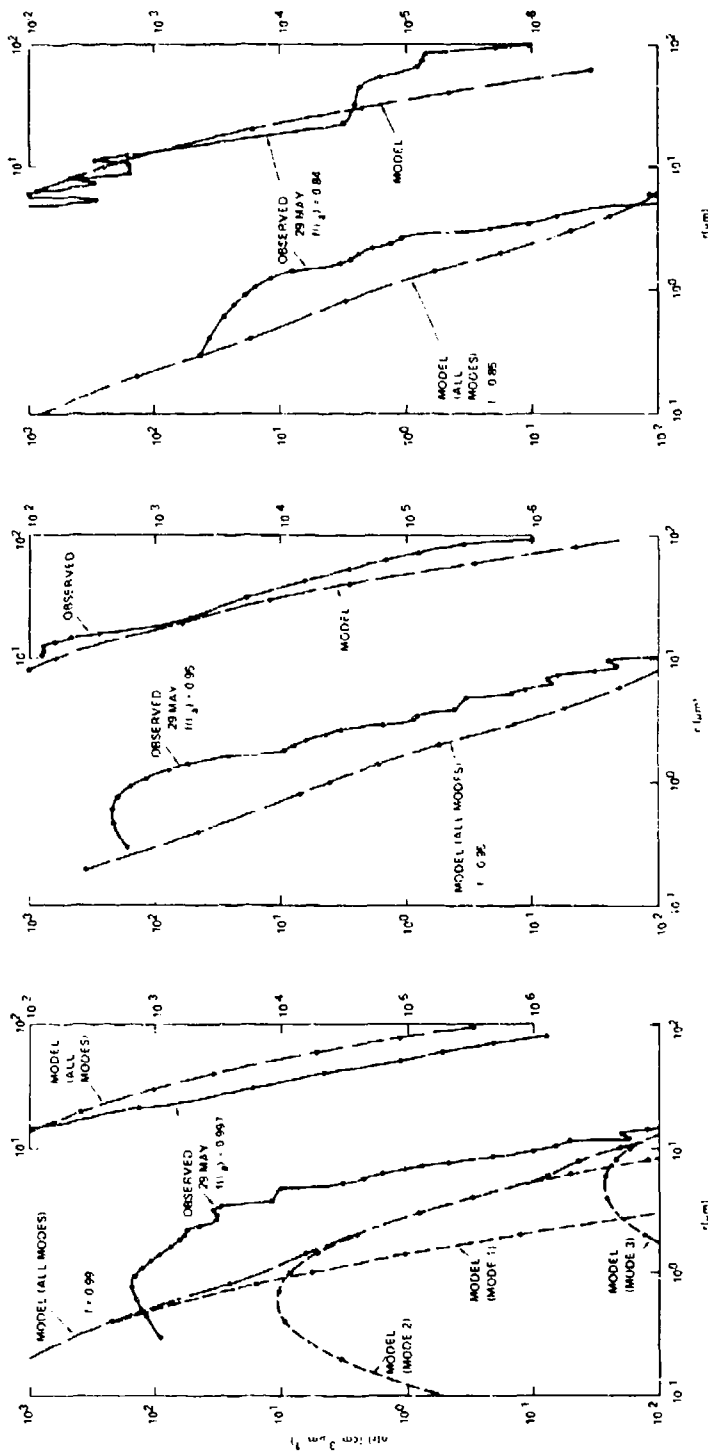


Figure 5. Modeled and observed (29 May) aerosol spectra. The all-mode model is for open ocean ($AM = 1$), with 4.1 m/s wind speed. The contribution of each mode of the model to $n(r)$ at an f of 0.99 is shown at the left.

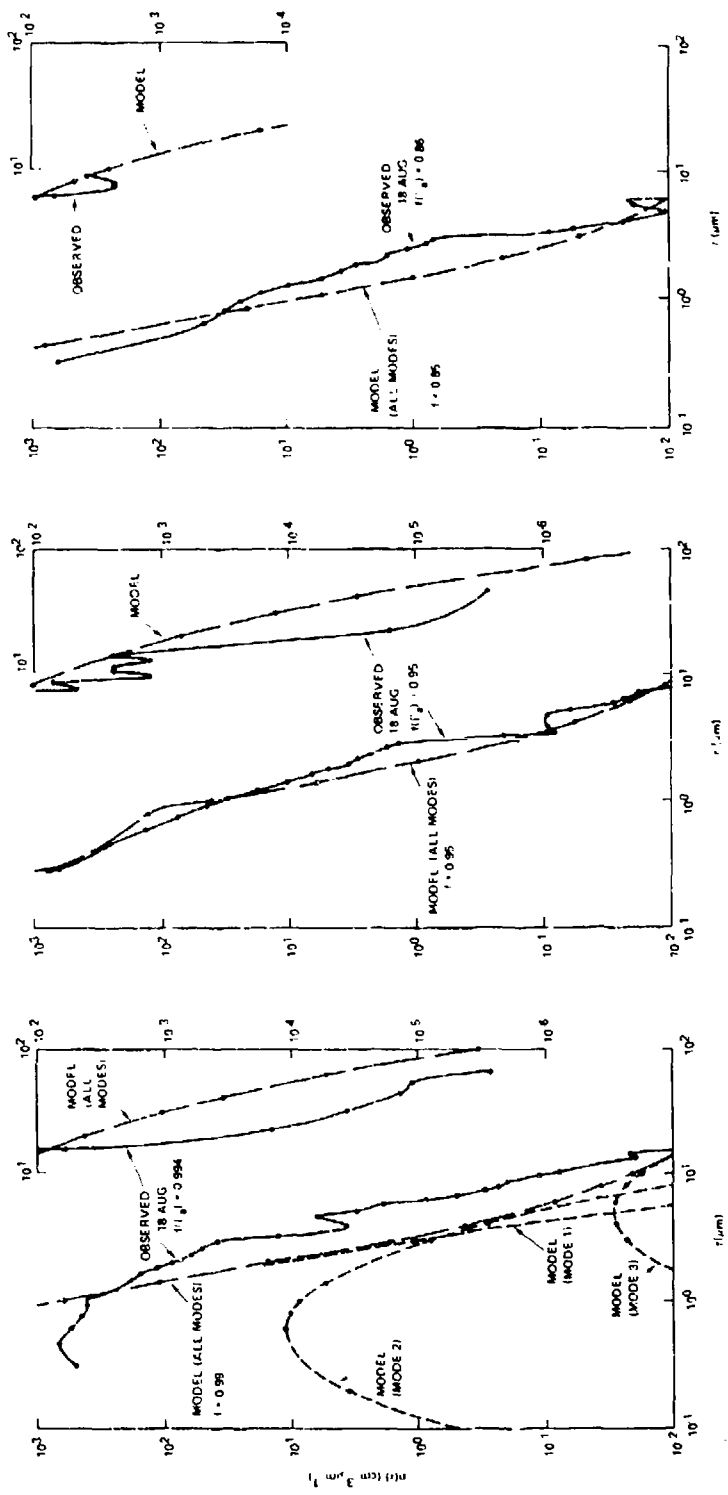


Figure 6. Modeled and observed (18 August) aerosol spectra. The all-mode model is for coastal (AM = 10) with 4.1 m/s wind speed. The contribution of each mode of the model to $n(r)$ at an $f(r)$ of 0.99 is shown at the left.

the region near $r = 3 \mu\text{m}$. For the same values of AM, w, w', and f, the modeled $n(r)$ approximates the observed $n(r)$ at $r = 7 \mu\text{m}$ and greatly overestimates the observed $n(r)$ at $r = 30 \mu\text{m}$. Apparently an increase in A_1 and A_2 is required to bring the modeled and observed values to about the same value in these radius bands.

The observed $n(r)$ had a mode in $n(r)$ at small r_s for large fs; whereas the model does not, unless A_1 can be assumed to vanish. This $n(r)$ modal characteristic has been observed by others (JG Hudson, University of Nevada, and EE Hindman, Colorado State University) and can be assumed to be real. Although the observations cannot provide information on $n(r)$ for $r < 0.23 \mu\text{m}$, the mode in $n(r)$ at small r and large f must be considered as an error source in the model if applied for above-surface marine-stratus conditions.

The modeled and observed $k(\lambda)$ s were almost identical for both months at $\lambda = 0.55 \mu\text{m}$ for $AM = 10$ and a wind speed of 4.1 m/s, although the model produces many more aerosols at small r_s . Apparently, in the determination of k for $\lambda = 0.55 \mu\text{m}$, the larger observed $n(r)$ in the region $0.4 \mu\text{m} \leq r \leq 10 \mu\text{m}$ compensated for the absence of small aerosols given by the model at much smaller r .

12. SUMMARY AND CONCLUSIONS

An analytical model recently formulated by the Navy (Gathman, 1983) specifies the extinction of optical radiation by water vapor and aerosols (equations 1, 2, and 3), for surface conditions. The controlling parameters are a 24-hour average surface wind speed, w, a current surface wind speed, w', an air mass factor, AM, and the relative humidity, f. The model was developed from somewhat limited surface data and is being refined as new data become available.

A recently acquired unique set of aerosol data beneath marine stratus clouds (Noonkester, 1982a, 1982b) was used to determine the capability of the model to specify the optical extinction coefficients, k, by aerosols beneath marine stratus (water vapor not included). The applicable elevations of the

model were established by assuming various vertical profiles of f , initially assumed to be adiabatic. Surface wind speeds w and w' given by the model (default value) were accepted as representing the stratus days. The stratus data were divided into two distinct air masses - marine ($AM = 1$) and continental ($AM = 10$) - on the basis of the average pressure patterns representing the days of measurements and aerosol spectra characteristics.

The model ks were compared with the ks calculated from the observed spectra for elevations where f is 0.99, 0.95, and 0.85; for $w = w' = 4.1 \text{ m/s}$; and for λ_s of 0.55, 3.75, and $10.59 \mu\text{m}$. Differences between the observed and model profiles of k were generally excessive for a near-adiabatic profile of f and the above values of w , w' , and AM . Differences remained excessive where unlikely profiles of f , unlikely values of w and w' , or intermediate values of AM were used. No combination of unlikely profiles of f , values of w and w' , or values of AM could be found that reduced the differences between the observed and model profiles of k to acceptable magnitudes (less than a factor of three) for most of the profiles of k . On the basis of these comparisons, it is concluded that without modification, the model is incapable of reproducing the observed ks produced by aerosols beneath marine stratus clouds.

Comparison of model and observed aerosol spectra, $n(r)$, (r is radius) revealed appreciable differences in many regions of r , assuming an adiabatic profile of f , $w = w' = 4.1 \text{ m/s}$, and AMs of 1 and 10. Reasonable changes in the profile of f , in w or w' , and in AM appeared incapable of significantly reducing the differences in all regions of r . The largest difference was in the region $1 \mu\text{m} < r < 10 \mu\text{m}$, where the observed $n(r)$ had many more aerosols at all r s, particularly for an AM of 1 (marine air mass). Without modifications, the model appears incapable of reproducing the observed aerosol spectra.

Similar comparisons should be made by analyzing stratus cloud data having reliable measurements of f , w , and w' . Methods are needed for establishing values of AM easily.

REFERENCES

- Fitzgerald JW, 1974, Effect of Aerosol Composition on Cloud Droplet Size Distribution: A numerical study, *J Atmos Sci*, vol 31, p 1358-1367.
- Gathman SG, 1983, Optical Properties of the Marine Aerosol as Predicted by the Navy Aerosol Model, *Optical Eng*, vol 22, p 57-62.
- Heaps MG, 1982, A Vertical Structure Algorithm for Low Visibility/Low Stratus Conditions, *Atmos Sciences Lab, White Sands Missile Range, Report ASL-TR-0111*.
- Houghton HG, 1951, On the Physics of Clouds and Precipitation, in *Compendium of Meteor*, TF Malone, editor, Am Meteor Soc.
- Hughes HG and DR Jensen, 1978, Extinction of IR Wavelengths by Aerosols in Coastal Fog, *Applied Optics*, vol 17, p 2138-2140.
- Jensen DR, 1980, Intercomparison of PMS Particle Size Spectrometers, NOSC TR 555.
- Lee IY, G Hanel, and HR Pruppacher, 1980, A Numerical Determination of the Evolution of Cloud Drop Spectra due to Condensation on Natural Aerosol Particles, *J Atmos Sci*, vol 37, p 1839-1853.
- McCartney EJ, 1976, *Optics of the Atmos*, Wiley.
- Neiburger M and CW Chien, 1960, Computations of the Growth of Cloud Drops by Condensation Using an Electronic Digital Computer, *Physics of Precipitation, Geophys Monograph 5 (NAS-NRC Pub 746)*, Am Geophys Union, p 191-210.
- Noonkester VR, 1980, Offshore Aerosol Spectra and Humidity Relations Near Southern California, preprint, Second Conf on Coastal Meteor, Los Angeles CA, Am Meteor Soc, p 113-120.
- Noonkester VR, 1982a, Aerosol and Humidity Structure Beneath Maritime Stratus Clouds: 1981 Data, NOSC TR 783.
- Noonkester VR, 1982b, Aerosol Spectra Observed in Maritime Stratus Cloud Layers, preprint, Conf on Cloud Physics, Chicago IL, Am Meteor Soc, p 87-90.
- Pinnick RG, SG Jennings, P Chylek, and HJ Auermann, 1979, Verification of a Linear Relation between IR Extinction, Absorption and Liquid Water Content of Fogs, *J Atmos Sci*, vol 36, p 1577-1586.
- Pruppacher HR and JD Klett, 1978, *Microphysics of Clouds and Precipitation*, D Reidel Publishing Co.
- Selby JEA, EP Shettle, and RA McClatchey, 1976, Atmospheric Transmittance from 0.25 to 28.5 μm , supplement LOWTRAN 3B, Air Force Geophysical Lab, Hanscom Field MA, Paper AFGL-TR-76-0258.

REFERENCES (cont)

Wells WC, G Gal, and NW Munn, 1977, Aerosol Distributions in Maritime Air and Predicted Scattering Coefficients in the Infrared, J Appl Meteor, vol 16, p 654-659.

APPENDIX A: COMPARISON OF MODELED AND OBSERVED $k(\lambda)$ PROFILES

DIFFERENCES WITHOUT ADJUSTMENTS OF $f(z^*)$ OR CHANGES IN w OR w'

Generally, the modeled $k(\lambda)$'s differ significantly from the observed. The modeled $k(\lambda)$'s for an AM of 1 differ more than those for an AM of 10, and the difference increases with an increase in elevation (greater f_s). Nevertheless, $k(\lambda = 10.59 \mu\text{m})$ at $f = 0.85$ is within a factor of 2 from the observed, for both AMs and both months.

$k(\lambda)$ AT THE SURFACE

The average observed f at the surface was 0.83 (at 31 m) for May and 0.81 (at 41 m) for August. These f_s are about 0.09 larger than expected in an adiabatic layer, assuming $f = 1$ at the cloud base. The modeled $k(\lambda)$'s for an f of 0.85 should represent the observed $k(\lambda)$'s at the surface, since the modeled $k(\lambda)$'s are somewhat insensitive to f for f_s near 0.80. Accordingly, the observed and modeled $k(\lambda)$ ($f = 0.85$) at $\lambda = 3.75 \mu\text{m}$ for August and at $\lambda = 10.59 \mu\text{m}$ for May were essentially equal. All other modeled $k(\lambda)$'s at $f = 0.85$ differed from the observed at the surface by factors greater than 3. Thus, the model does not appear capable of specifying the $k(\lambda)$'s at the surface; adjustments of w and w' cannot cause the modeled $k(\lambda)$'s to approach the observed within a factor of 3 for all λ 's and both months simultaneously.

The model specifies larger $k(\lambda)$'s at the surface during August, whereas the observed profile indicates the opposite relation. As shown below, no reasonable change in the model parameters will produce the observed profile.

COMPARISON WITH CHANGES IN $f(z)$

No change in $f(z)$ could make the modeled k approach the observed either at a λ of 0.55 (considering only AM = 1) for both months or at a λ of 3.75 μm for May. If the elevation at which $f = 1$ were decreased by 50 to 80 m, the modeled profile of $k(\lambda)$ would approximate the observed for $\lambda = 3.75 \mu\text{m}$ during August and for $\lambda = 10.59 \mu\text{m}$ during May. Such a change in the elevation of

saturation is not reasonable. No reasonable change in $f(z)$ would cause the modeled $k(\lambda)$ to approximate the observed at all levels, for all λ s, and for both months when the wind speed is 4.1 m/s, simultaneously.

COMPARISON WITH LARGER w AND w'

If both w and w' are 10.3 m/s (20 knots) and $AM = 1$, curve C for $\lambda = 0.55 \mu\text{m}$ (in main text figure 4) is generated. This profile of $k(\lambda)$ differs from the observed by more than a factor of 3 at fs of 0.99 and 0.95 and by less than a factor of 3 at f of 0.85. For λ s of 3.75 and $10.59 \mu\text{m}$, curve C is for w and w' values of 10.3 m/s and an AM of 10. These curves approximate the observed at all fs for $\lambda = 3.75 \mu\text{m}$ in August, approximate the observed for $\lambda = 3.75 \mu\text{m}$ at $f = 0.85$ for May, approximate the observed for $\lambda = 10.59 \mu\text{m}$ at $f = 0.95$ for May, and approximate the observed for $\lambda = 10.59 \mu\text{m}$ at $f = 0.99$ for August. The difference is excessive for $fs \gtrsim 0.88$ at a λ of $10.59 \mu\text{m}$ for both months. Thus, a change of wind speed will not cause the modeled $k(\lambda)$ to approximate the observed at all levels, for all λ s, and for both months, simultaneously, when the humidity profile is adiabatic below the cloud base.

COMPARISONS WITH ADJUSTMENTS IN $f(z^*)$, w , AND w'

If the elevation at which $f = 1$ were decreased by 50 to 70 m, curve C in figure 4 would approximate the observed $k(\lambda)$ at $\lambda = 0.55 \mu\text{m}$ for both months and at $\lambda = 3.75 \mu\text{m}$ for May. Such a change for the remaining three λ -month combinations would increase to excessive magnitudes the differences between the modeled and observed profiles. No combination of simultaneous adjustments in $f(z^*)$, w , and w' will cause the modeled $k(\lambda)$ s to approximate the observed $k(\lambda)$ s at all λ s and for both months.